

**Wojciech Bartz\*, Jacek Kościuk\*\*, Maria Gašior\*\*\*,  
Teresa Dziejcz\*\*\*\***

## *Petrographic, mineralogical, and climatic analyses, and risk maps for conservation strategies*

### *Analizy petrograficzne, mineralogiczne i klimatyczne oraz mapy ryzyka dla strategii konserwatorskiej*

#### *Introduction*

El Fuerte de Samaipata is a pre-Hispanic archaeological site in Bolivia, in the province of Florida and the department of Santa Cruz, on the eastern slopes of the Andes at an altitude ca. 1890–1925 m. Due to its historical and cultural value, the site was inscribed on the UNESCO World Heritage List in 1998.

The entire archaeological site covers about 40 hectares and consists of two main parts:

- An administrative and ceremonial complex of ca. 50 buildings typical of provincial Incan architecture located in the southern part of the site;
- A natural rock (ca. 80 × 250 m) towering over the Piray valley in the northern part of the site.

The natural rock was the main subject of the project “Architectural examination and complex documentation of Samaipata (Fuerte de Samaipata/Bolivia) site from the World Heritage List”, of which this study is a small excerpt.

The whole rock is densely covered with a complex arrangement of terraces, platforms, water reservoirs, and channels. Between them are numerous petroglyphs depicting animals or geometric forms. The present form of the rock is the result of the activities of various local cultures over almost 1200 years, who treated the rock as a sacred place (*wak'a*). However, Incan characteristics clearly dominated this rock after it was incorporated into the Inca Empire (*Tawantinsuyu*) in the 2<sup>nd</sup> half of the 15<sup>th</sup> century.

Apart from the 16<sup>th</sup> century mentions by Spanish chroniclers [1] and a short description from the 1<sup>st</sup> quarter of the 19<sup>th</sup> century by Alcide Dessaline d'Orbigny [2], the site only became a subject of systematic scientific interest in the 20<sup>th</sup> century [3], [4]. The range of studies significantly increased in 1970 due to the establishment of the Archaeological Research Centre in Samaipata [5] and research by German scholars [6]–[11].

#### *Outline and main aim of the study*

In the last quarter of the 20<sup>th</sup> century, intensive research combined with the removal of vegetation growing on the rock and the accumulated organic layers led to the exposure of the entire ridge of the rock (Figs. 1A, B). This not only enabled detailed research to be conducted on previously unavailable parts of the whole complex, but also contributed to the popularisation of El Fuerte as an important tourist attraction.

The acceleration of rock erosion was an unforeseen side effect of this exposure. The rapidly progressing ero-

\* ORCID: 0000-0002-7267-2776. Institute of Geological Sciences, University of Wrocław, e-mail: wojciech.bartz@uwr.edu.pl

\*\* ORCID: 0000-0003-0623-8071. Faculty of Architecture, Wrocław University of Science and Technology.

\*\*\* ORCID: 0000-0002-9152-3792. Ceramics and Glass Conservation and Restauration Department, Eugeniusz Geppert Academy of Art and Design in Wrocław.

\*\*\*\* ORCID: 0000-0003-2855-0074. Faculty of Architecture, Wrocław University of Science and Technology.



Fig. 1. The southern slope of the rock:  
 A – during the time of research by Erland Nordenskiöld (around 1923) (photo from archives of the Samaipata Archaeological Research Centre);  
 B – in April 1974 (photo courtesy of Damiano Montenegro Fernández)

sion of the rock makes petroglyphs less and less clear, and some are no longer recognisable.

The first attempts to address the problem of erosion go back to the beginning of the 21<sup>st</sup> century, but the problem is complicated due to the nature and the size of the rock itself, and it has not yet been satisfactorily resolved. Research has focused mainly on mineralogical and petrographic analyses of the rock and finding suitable consolidators, recipes for putties to seal natural cracks, and methods to stop the spread of mosses, lichens, and algae [12]. Much less attention has been paid to a holistic view of the problem, and in particular to determining all risk factors conducive to erosion and drawing up risk maps identifying the most vulnerable areas requiring immediate conservation intervention. This subject, in addition to complementary mineralogical and petrographic research, is the main topic of this study.

### *Methodology and methods*

Apart from anthropogenic factors, the most significant reasons for the progressing erosion of the rock are climatic and biological hazards. Depending on the rock properties and susceptibility to individual threats, each of these factors will interact with the rock differently. Therefore, it is important to thoroughly understand all the properties of the rock – physical, chemical, and mineralogical, and at the same time to identify all risk factors.

The methodology adopted in these studies was to examine each of these factors separately, and then to analyse the obtained results to understand how they interact. Climatic factors directly affecting the rock include aeolian processes (wind erosion), thermal shock effects, and precipitation. Biological factors include the effects of plant vegetation and the spreading of lichens and algae. The

shape of individual parts of the rock also needs to be considered – this can either intensify the effects of risk factors or minimise them. Particularly important is the inclination of slopes and their orientation towards cardinal compass directions, areas of natural and anthropogenic infiltration of rainwater (cracks, holes, etc.), zones of permanent accumulation of rainwater (artificial reservoirs and natural depressions), zones of water effluence, and deposits of organic material favourable for plant vegetation. Due to this, accurate data obtained by 3D laser scanning of the whole rock<sup>1</sup> and photogrammetric documentation<sup>2</sup> has been very important.

### *Analysis of the current state of erosion*

The mutual interaction of all risk factors and the local properties of heterogeneous sedimentary rock has resulted in different types of erosion – peeling, cracking, exfoliation, and powdering. During the two seasons of fieldwork (2016, 2017), the main stages of erosion and areas of occurrence were identified.

The first stage of erosive phenomena is micro-cracks appearing on the rock surface (Fig. 2A). Their presence can potentially be associated with thermal shock and the alternation between the soaking and drying of porous rock. Practically, 50% of the Samaipata rock surface is covered with such micro-cracks (Fig. 2B).

<sup>1</sup> Cf. J. Kościuk, B. Ćmielewski, M. Telesińska, A. Kubicka, *3D terrestrial laser scanning of El Fuerte de Samaipata*, in the same issue of “Architectus”.

<sup>2</sup> B. Ćmielewski, I. Wilczyńska, C. Patrzalek, J. Kościuk, *Digital close-range photogrammetry of El Fuerte de Samaipata*, in the same issue of “Architectus”.

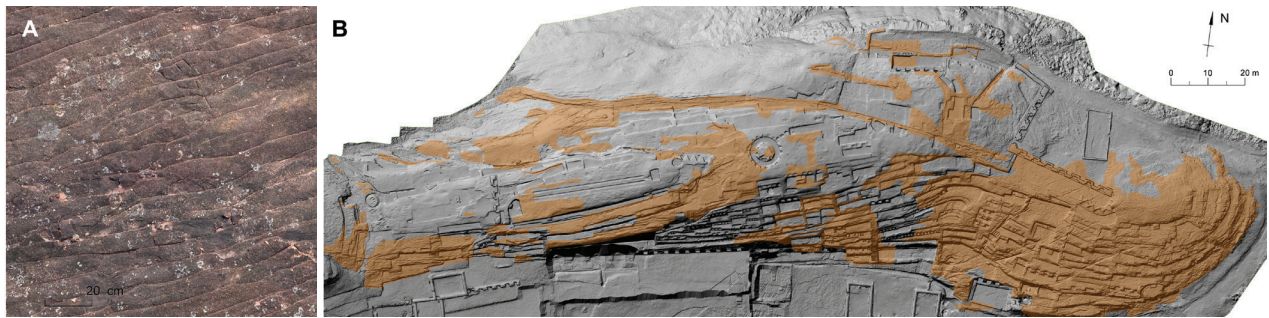


Fig. 2. First stage of erosion:

A – an example of the first phase of erosion (micro-cracks) on 0.3 mm-resolution orthoimage (photo by J. Kościuk);  
 B – areas of numerous micro-cracks in the lithic surface (elaborated by T. Dziedzic)

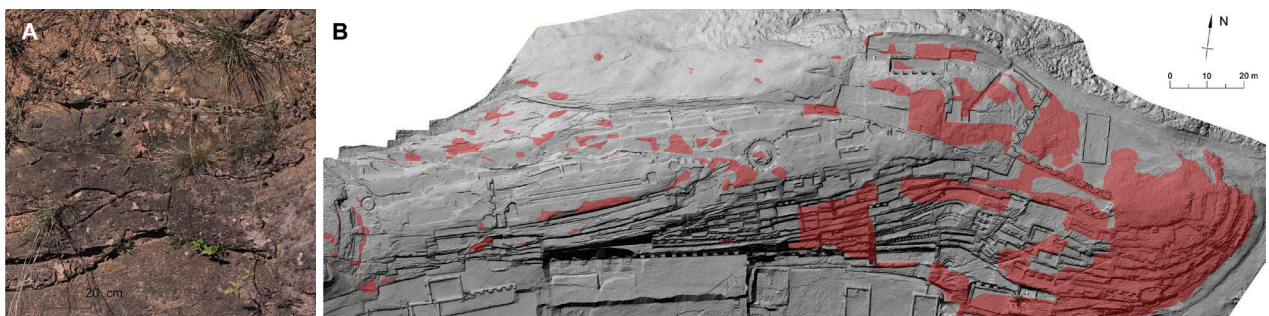


Fig. 3. Second stage of erosion:

A – an example of the second phase of erosion (exfoliation) on 0.3 mm-resolution orthoimage (photo by J. Kościuk);  
 B – areas of exfoliation of the lithic surface (elaborated by T. Dziedzic)

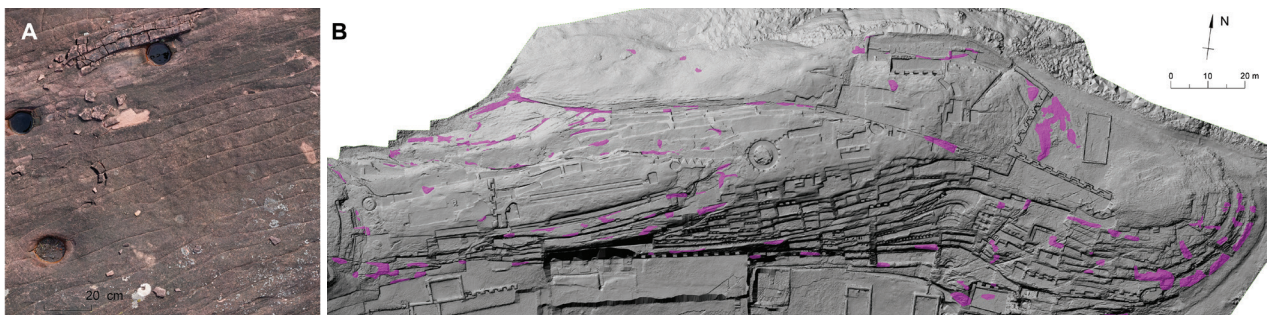


Fig. 4. Third stage of erosion:

A – an example of the third phase of erosion (loose fragments of the rock lying on the surface) on 0.3 mm-resolution orthoimage (photo by J. Kościuk);  
 B – zones of loose lithic material (elaborated by T. Dziedzic)

The second observed erosion stage, especially where the natural stratification of the rock is oblique in relation to its surface, is exfoliation – individual layers separate from the bedrock (Fig. 3A). Exfoliation processes are accelerated by the presence of vegetation whose root system penetrates and breaks existing micro-fissures. It is estimated that about 25% of the entire rock surface is at risk of exfoliation (Fig. 3B). A strong correlation is visible between the zones of micro-cracks and the zones where the surface layers of the rock are exfoliating.

In the third stage of erosion, detached fragments of rock completely lose contact with the ground and begin to move (Fig. 4A). The progression of this process causes their further fragmentation into ever smaller pieces that are easily

moved by rainwater and wind. Accumulating deposits of such material, additionally enriched with organic particles blown by the wind, are an excellent breeding ground for growing plants whose root system will penetrate the rock deeper and deeper. Zones in which loose lithic material is deposited (Fig. 4B) are increasing every year.

### *Climatic and topographical factors*

El Fuerte de Samaipata is located in the southern hemisphere at 18° latitude – in the zone between the equator and the Tropic of Capricorn. This fact is essential for considering the impact of climatic factors on possible conservation hazards, mainly since the main ridge of the rock

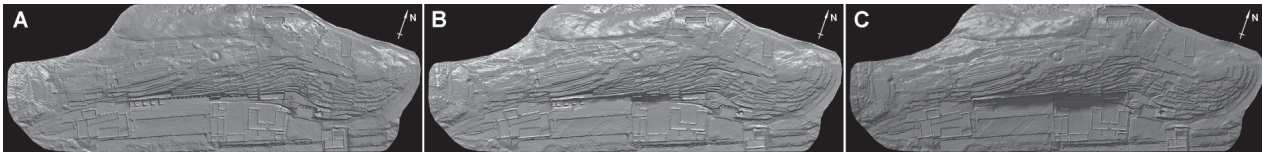


Fig. 5. Samples of visualisations of the rock insolation on 21<sup>st</sup> June for the fourth (A), sixth (B), and eight (C) hour of daylight (elaborated by J. Kościuk)

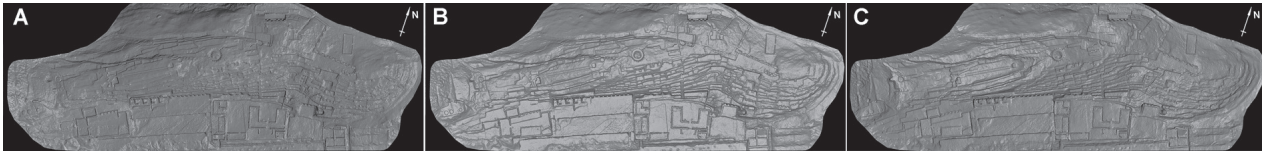


Fig. 6. Samples of visualisations of the rock insolation on 21<sup>st</sup> December for the fourth (A), sixth (B), and eight (C) hour of daylight (elaborated by J. Kościuk)

is latitudinally oriented. Strong rays of sun heat both the northern and the southern slope of the hill. The combination of this with the 24-hour cycle of temperature changes and cold winds creates the risk of thermal shock. Identification of areas where such risk may occur was, therefore, a priority for this study.

The first step in this type of analysis was to determine which fragments of the complex surface of the rock are most exposed to sunlight. These types of calculations are usually carried out to determine the energy balance of a building, or to assess the possibility of using photovoltaic cells. Software for this kind of simulation, for example, EnergyPlus, uses integrated meteorological data – EPW files that contain information about the temperature and intensity of solar radiation (direct and diffused). However, there is no weather station on El Fuerte de Samaipata or even in the town of Samaipata itself; hence, there is no detailed meteorological data for this place that would allow cumulated solar energy to be calculated. The problem had to be solved differently.

In our case, we were not interested in the absolute values of accumulated solar energy expressed in  $W \cdot h/m^2$ , but only the relative differences in the insolation of individual parts of the rock. Therefore, instead of calculating the energy balance, a virtual 3D model of the whole hill was used. The model was embedded in the virtual 3D space according to geographical coordinates and correctly oriented towards north. The two most opposing moments of the solar year were selected – summer solstice (21<sup>st</sup> June) and winter solstice (21<sup>st</sup> December). At equal intervals corresponding to daylight hours, ten visualisations were rendered for 21<sup>st</sup> June (Fig. 5) and twelve for 21<sup>st</sup> December (Fig. 6). The rendering tool used was Bentley MicroStation V8i software (version 08.11.09.459), which enables the realistic visualisation of solar lighting according to geographical location and specific date. The values of the horizontal and vertical angles of incidence of sunlight were additionally verified using Stellarium software (version 0.16.0). As a rendering algorithm, ray tracing was selected, which also includes diffused light and ground reflection for skylight, as well as cloud cover (cloudless

conditions were selected) and air transparency (due to the high humidity of air in this region of Bolivia, the option “rural” was chosen).

Grey-scale visualisations for individual hours of daylight were then stitched together into one image, separately for 21<sup>st</sup> June and 21<sup>st</sup> December, and the resulting images were divided into six classes of grey. Each of the grey classes was assigned one of six basic colours from red for the most illuminated surfaces throughout the whole day, to blue for those that remain mainly in the shadows. In this way, maps were obtained showing to some extent which fragments of the rock could have warmed up the most at these two different moments of the year (Figs. 7, 8), so zones in which one could expect thermal shock due to the rapid temperature changes between day and night.

During our stay on El Fuerte in June–July 2016 and 2017, we repeatedly experienced such temperature jumps. At the end of the workday, the rock was heated in many places to almost 40 °C, while the next morning it was covered with frost and ice.

The effect of thermal shock is intensified by strong winds blowing over El Fuerte. The specificity of the terrain, with its parallel ranges of mountains and valleys (Figs. 9A, B), means that NNW winds dominate there (Fig. 9C).

Precipitation is another essential factor from the point of view of conservation hazards. The annual rainfall for the nearby town of Samaipata reaches 1000 mm – for comparison, this is almost twice as much as for London. For El Fuerte, located nearly 300 m higher than the town, annual rainfall is undoubtedly even higher, but detailed meteorological data are not available.

The virtual 3D model of the rock was used again to simulate the influence of wind on the effect of thermal shock. The model was illuminated from a NNW direction (335° from the north) and rendered using the same software. In this way, the most illuminated parts of the hill simulated the surfaces most exposed to the wind, and thus those that cooled down the fastest (Fig. 10). This chart is also an approximate image of the zones where wind erosion effects may occur.

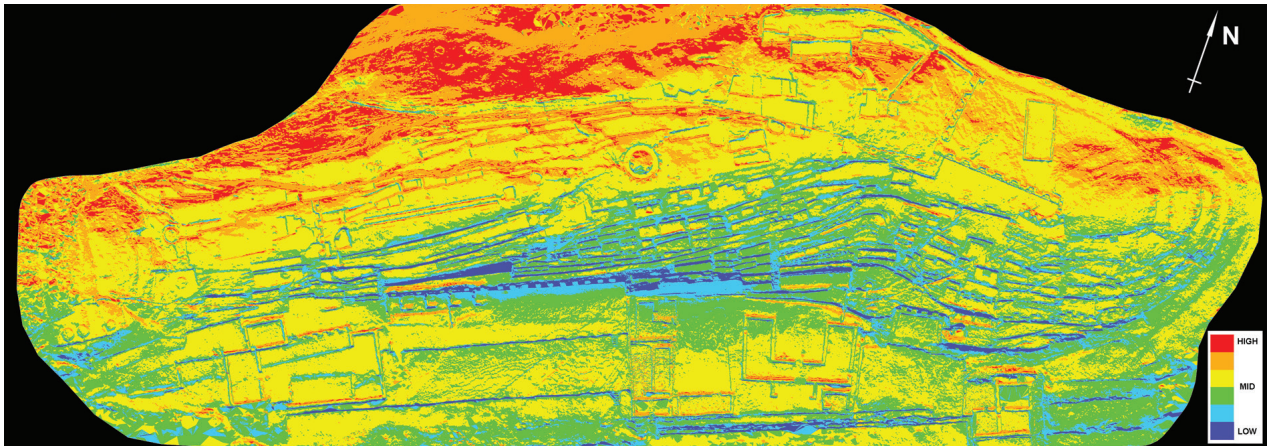


Fig. 7. Rock insolation on 21<sup>st</sup> June (elaborated by J. Kościuk)

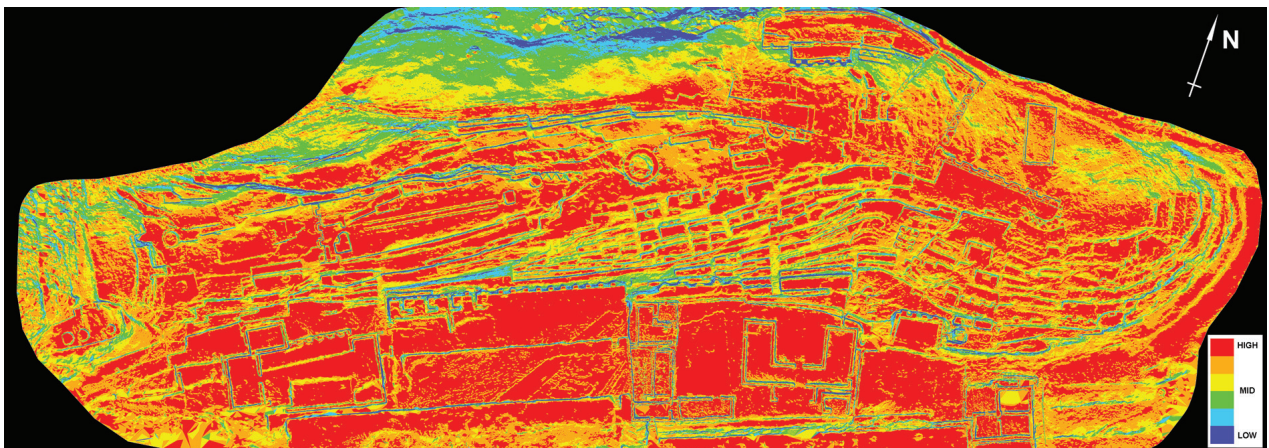


Fig. 8. Rock insolation on 21<sup>st</sup> December (elaborated by J. Kościuk)

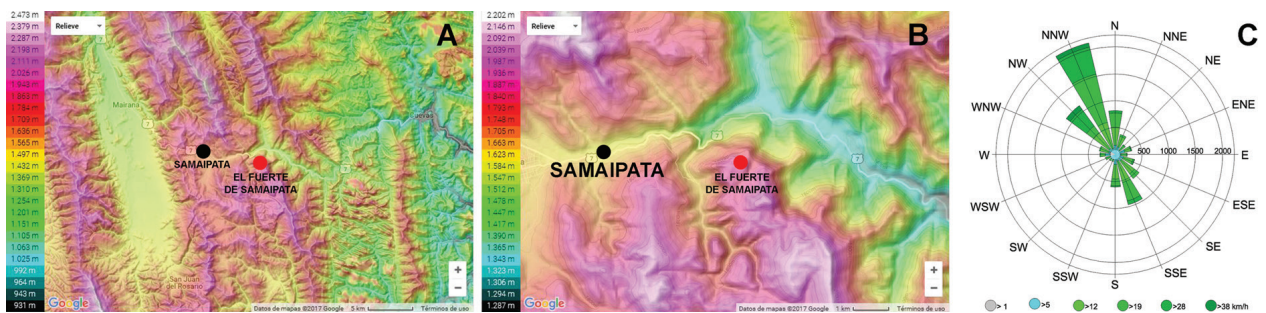


Fig. 9. The topographical situation of El Fuerte de Samaipata (A and B) and the wind rose (C)

(sources: <http://suncalc.net>; [https://www.meteoblue.com/en/weather/forecast/modelclimate/samaipata\\_bolivia\\_11494517](https://www.meteoblue.com/en/weather/forecast/modelclimate/samaipata_bolivia_11494517) [accessed: 12.01.2018])

Threats related to atmospheric precipitation are two-fold. Rainwater that accumulates on the rock surface for a long time causes hydrolysis and the subsequent washing-out of the binder of the sandstone rock. If the temperature drops below 0 °C, water freezing in the rock crevices will break them. Fortunately, the months with the highest rainfall (December to March) are also the warmest, when the temperature usually does not fall below freezing point. In both cases, however, the decisive factor influencing the

possible retention of rainwater is the inclination of the slope and the occurrence of local depressions.

Fortunately, one of the thematic styles of displaying 3D objects in Bentley MicroStation V8i is slope inclination. With this, as in all previous cases, the results were divided into six classes using a colour scale in which the red corresponded to surfaces where the inclination did not exceed 8°, and the blue meant a slope greater than 75° (Fig. 11).

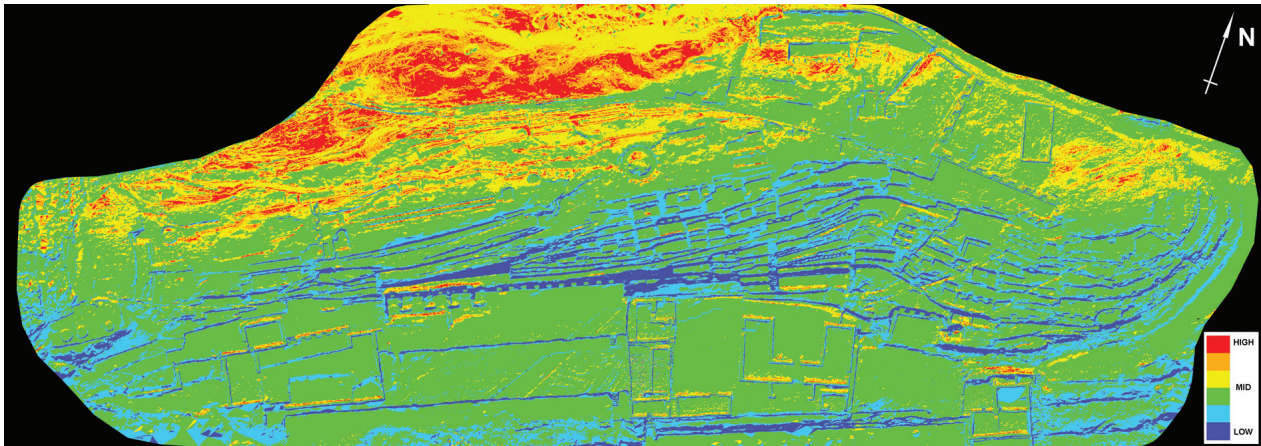


Fig. 10. Exposure to the prevailing wind direction (elaborated by J. Kościuk)

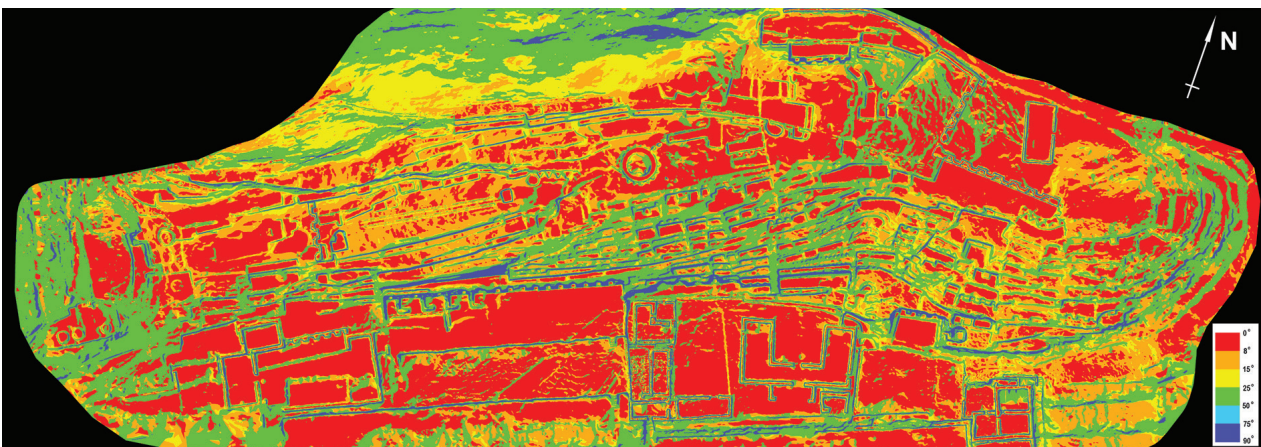


Fig. 11. Slope inclination analysis (elaborated by J. Kościuk)

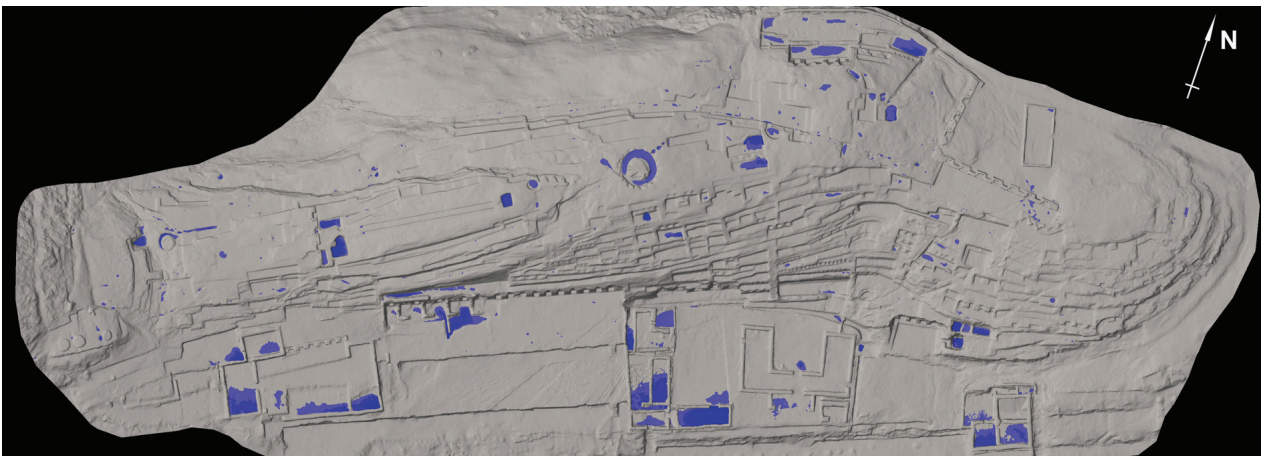


Fig. 12. Depressions without drainage (elaborated by J. Kościuk)

Local depressions were also searched for in the Bentley MicroStation V8i environment – contour lines were generated every 10 cm and those that formed enclosed areas were selected (Fig. 12). The results were presented this time in a different colour scale. The results of all these partial analyses were further used to prepare risk maps for conservation strategies.

### ***Biologically induced erosion***

In addition to the climatic and topographic aspects mentioned above, biological factors also promote rock erosion. The scope of the entire project did not include genetic testing, which would have required the separate consent of the Bolivian Ministry of the Environment. Biological factors



Fig. 13. Examples of various forms of plants, lichens, fungi, and algae growing on the rock surface (photo by J. Kościuk)

have also already been the subject of partial studies conducted by Sonia Avilés [12]–[14]. Nevertheless, numerous plants growing on the rock, as well as lichens, mosses and algae (Fig. 13), distract not only for aesthetic reasons, but mainly due to their impact on erosion. This impact is not only the already mentioned process of breaking micro fissures by penetrating plant roots, but also the biodegradation of the binder of the fine sandstone particles, which is even more invasive.

### *Mineralogical and petrographic analyses*

Mineralogical analyses were done for 10 samples taken from the Samaipata rock and one sample of locally occurring clay material that is used for restoration and filling cavities in the Samaipata rock. The rock material was split into two portions with a stone cutting saw. Afterwards, all samples were laboratory dried at temperature of ca. 40 °C, to a constant weight. The first halves were impregnated with a low

viscous epoxy-resin under vacuum conditions and used for the preparation of a petrographic thin section according to procedure described by Jan Elsen [15]. Petrographic analyses were performed using a Zeiss Axiolab polarising microscope.

The second halves were analysed by means of

- powder X-ray diffraction (XRD);
- thermal analysis (DSC-TG);
- scanning electron microscopy (SEM-EDS).

In the latter case, analyses were performed for two representative samples (polished thin sections, 30 nm carbon coat) chosen on the basis of petrographic observation. A Jeol JSM IT-100 scanning electron microscope (SEM) equipped with an Oxford EDS system operating at an acceleration voltage of 16 kV was used.

XRD and DSC-TG analyses were done on a sieved fraction of <63 μm that mostly contained rock cement. XRD measurements were taken with a Siemens D 5005 diffractometer, using Bragg–Brentano geometry and Co K $\alpha$

radiation, in the 2Theta range  $4\div 75$  deg. DSC-TG analysis was carried out with a PerkinElmer STA 6000 thermal analyser, from  $40\text{ }^{\circ}\text{C}$  up to  $999\text{ }^{\circ}\text{C}$ , at a constant heating rate of  $15\text{ }^{\circ}\text{C}/\text{min}$  in  $\text{N}_2$  atmosphere.

The sample of the locally occurring clay was powdered and suspended in ca. 500–700 ml of distilled water. Afterwards, it was allowed to settle gravitationally (12 hours) to sediment most of the particles not part of the clay fraction (greater than ca.  $4\text{ }\mu\text{m}$  in diameter). Subsequently, the cloudy supernatant was siphoned and then centrifuged at 5000 rpm for 10 min. The obtained centrifuged sediment was used to prepare three oriented mounts. For each one, a few drops of the suspended clay sample were placed onto a slide using a pipette, and the slides were left to dry. Finally, the first slide was saturated with ethylene glycol, the second one was heated for one hour at  $550\text{ }^{\circ}\text{C}$ , and the last one was left untreated. XRD measurements were made using a B Siemens D 5005 diffractometer with Bragg–Brentano geometry and  $\text{Co K}\alpha$  radiation in the 2Theta range  $4\div 35$  deg.

### Results and discussion

The research was intended not only to identify the sources of conservation risks, but also to determine their

potential scope. To this end, a number of risk maps were developed, and physicochemical, mineralogical, and petrographic analyses were used to characterise the local sandstone and determine its weak points.

#### *Climatic and topographical analyses*

The juxtaposition of insolation data (Figs. 7, 8) with simulations of exposure to prevailing winds (Fig. 10) determined the zones for which there is the greatest risk of thermal shock. For the June solstice, these are mainly the northern slopes of the hill and all surfaces of niches, terraces, and platforms with northward exposure (Fig. 14).

It should be clearly stated here that the presented risk scales do not use absolute values. This is particularly important when comparing June data with December data. The risk of negative temperatures on El Fuerte appears mainly in June, July, and August, and these are the months in which the lowest maximum temperatures are recorded. Together with September, this is also the period of the strongest winds. Temperatures dropping below zero and strong winds are the two most important factors for the risk of thermal shock during this period of the year.

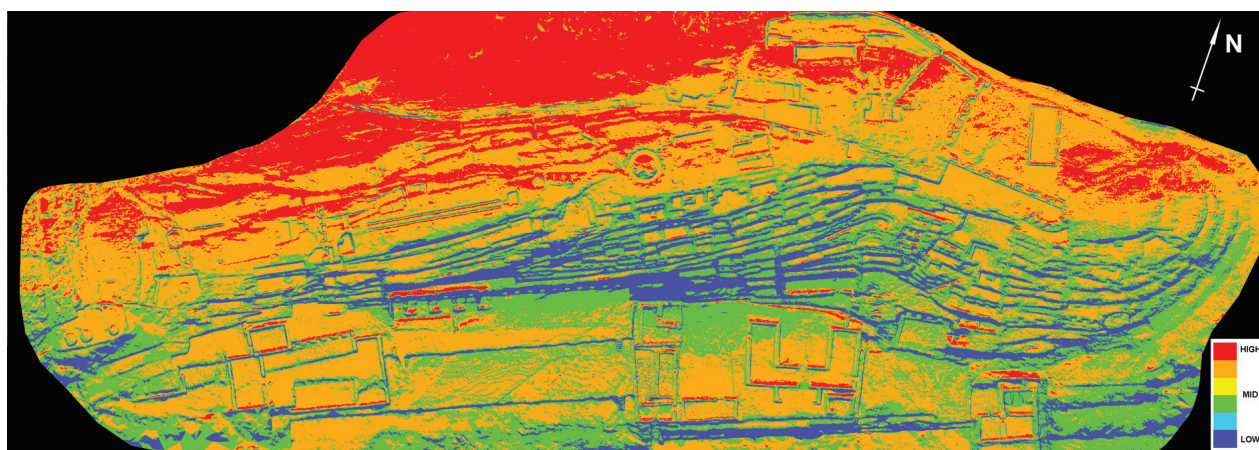


Fig. 14. Risk of thermal shock on 21<sup>st</sup> June (elaborated by J. Kościuk)

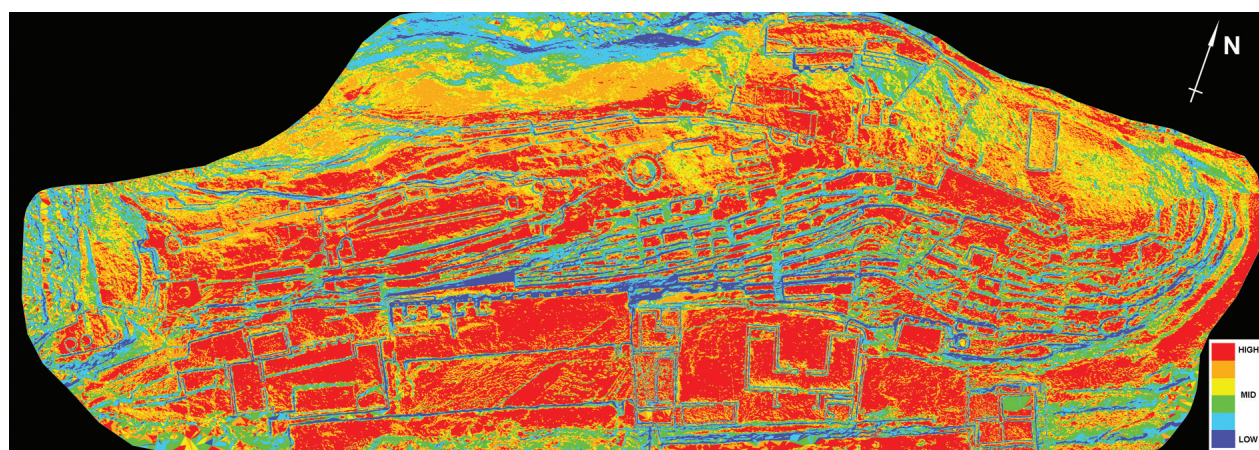


Fig. 15. Risk of thermal shock on 21<sup>st</sup> December (elaborated by J. Kościuk)

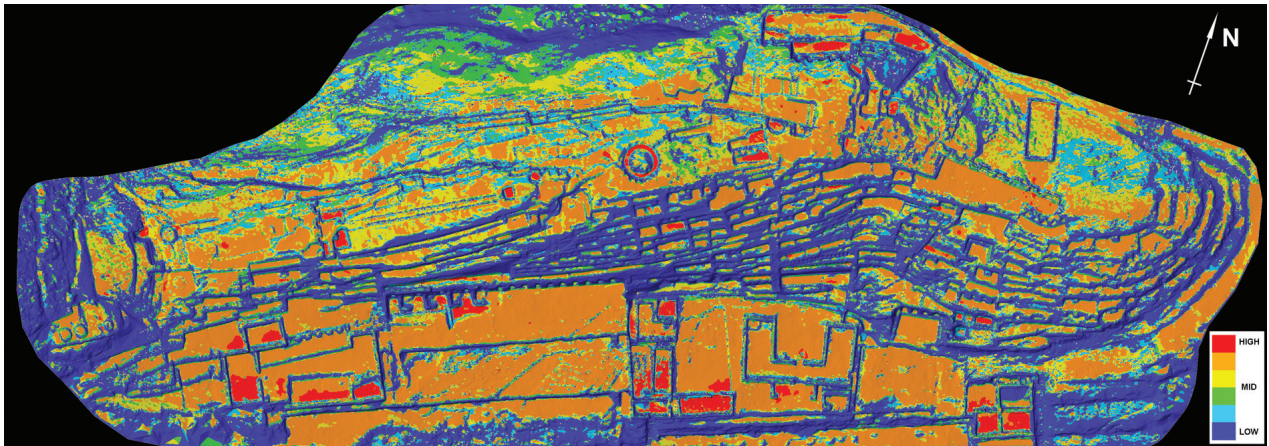


Fig. 16. Accumulated risk factors: slope inclination, depression, thermal shock, wind erosion (elaborated by J. Kościuk)

Risks of thermal shock for the December solstice are completely different. Mainly all horizontal surfaces are threatened, and on slopes, even southern ones, the risk is much lower (Fig. 15).

In turn, mid-November to mid-March is a period when the minimum temperature does not fall below zero. The winds are also much weaker, but the maximum temperatures are among the highest in the year. An important factor is also the difference in the angle of incidence of sunlight. From November to March, at these latitudes, in the middle of the day, the sun's rays fall almost perpendicularly, so all horizontal surfaces heat up much more strongly. Risk levels defined as "high" for June and December are therefore hardly comparable.

The risk of thermal shock is not the only threat to El Fuerte. The previous section also specified the impact of wind erosion (Fig. 10), slope inclination (Fig. 11), and local depressions (Fig. 12). Summing up these four factors gives us a full picture of the threats caused by climatic factors and the site topography. The resulting map of accumulated risk factors (Fig. 16) indicates that, apart from local depressions that were already discussed separately, the most negative factors add up on all horizontal areas. Therefore, from this point of view, conservation priorities should focus on these areas, and particularly on all petro-

glyphs located there. This, however, does not exhaust the list of all hazards regarding El Fuerte.

#### *Biologically induced erosion*

El Fuerte de Samaipata is a red sandstone rock with high porosity. It contains iron compounds, which affect both its colour and resistance to weathering. It is a rock uplift exposed to destructive atmospheric factors: chemical, mechanical, and physical. Most processes are initiated in the presence of water in various forms (rainfall, fog, and condensation). Wind and associated abrasion processes are also highly destructive.

All these factors affect the intensive weathering of the rock. There are deep cracks in sandstone in many places. The largest run diagonally from the north-west to the south-east.

The rock is covered with reliefs of varying heights. Due to the presence of artificial (reliefs with symbolic decoration) and natural depressions, there are numerous deposits where water, loose rock fragments, and organic material deposited by the wind collect. The accumulation of humidity and organic material creates favourable conditions for the development of lichens, and as a consequence of their soil-forming activity, also the growth of higher vegetation and mosses (Fig. 17). These plants are

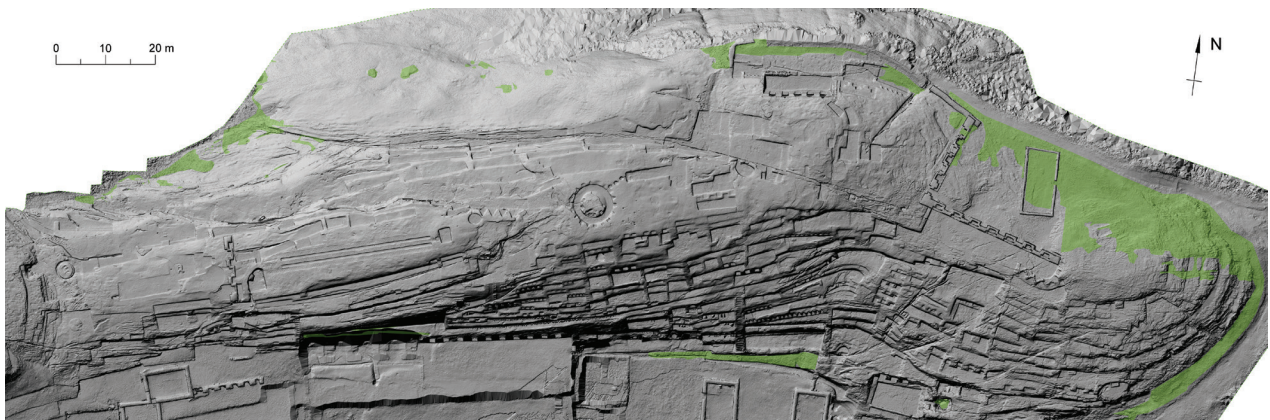


Fig. 17. Green plant zones (elaborated by T. Dziedzic)

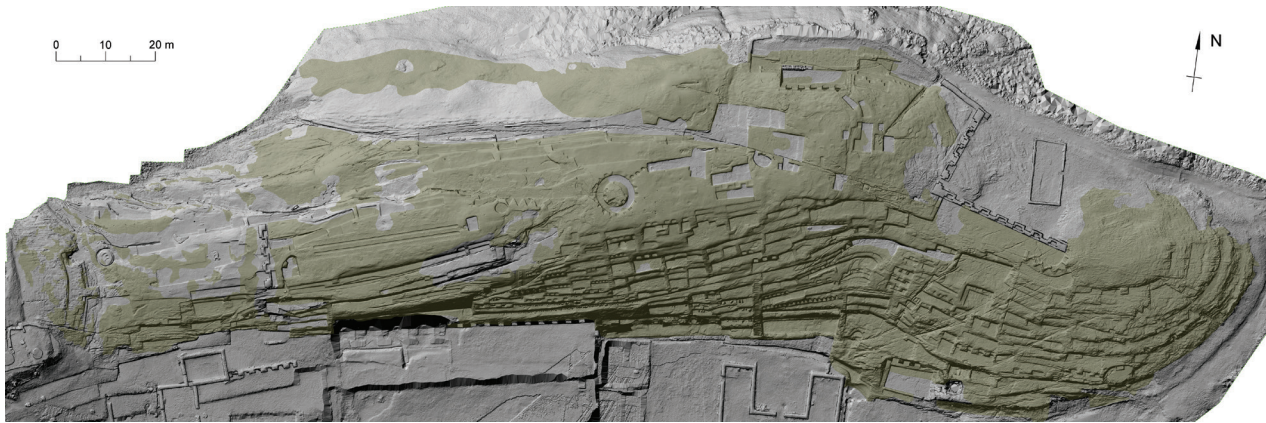


Fig. 18. Zones of intensive occurrence of lichens, fungi, and algae (elaborated by T. Dzedzic)

strongly rooted. Attempts to remove them can damage the rock, and root expansion leads to the cracking and breaking of the rock.

The growth of numerous types of fungi, algae, and lichens including *Lecanora*, *Cladonia*, *Aspicilia*, *Xanthoria*, and *Rhizocarpon* is observed on most of the rock surface (Fig. 18). Lichens cause moisture in the sandstone to be retained, create colourful spots on the entire surface of El Fuerte, and the acids they produce cause rapid progressive chemical erosion of the rock [16].

Lichens have a particularly destructive effect, as they form spots that are crusty and very stiff. Their presence causes not only drastic colour changes, but also the transformation of the stone structure and, as a consequence, the powdering and flaking of the surface attacked by them. This type of lichen is observed on the surface of El Fuerte in the northern part, and is particularly abundant in one of the most valuable parts of the monument – within the relief that depicts the “Big Snake” (the rattlesnake) and on the surface of what is known as the “Choir of Priests”.

On the surface of the El Fuerte rock, there are also relatively numerous traces of vandalism. These are mainly inscriptions carved in rock of various sizes and locations.

Fortunately, since the introduction of restrictive regulations that prohibit climbing on the rock, such activities are no longer recorded.

The greatest damage is observed in the eastern and southern parts of the rock. Damage in the eastern part is mainly caused by exposure to wind and abrasion and rainwater and its associated washing and rinsing of the sandstone surface. In the southern part, the vertical surface of the rock is destroyed, which is probably related to the action of water accumulating in the rock structure and just leaking on the southern slope of the hill.

On the northern slope of the rock, in a place invisible to visitors, next to similar samples already made by Sonia Avilés, an attempt was made to mechanically clean the surface of the rock from lichens, fungi, and algae using soft brushes and distilled water. The cleaned surface was impregnated with Biotin biocide 40% (solution in a mixture of ethyl and isopropyl alcohol).

The next test was carried out on a crude, lichen-covered piece of rock, which was impregnated with Biotin R biocide alcohol solution (manufactured by CTS, Italy) in various concentrations: 10%, 20%, and 40%.

It was observed that the application of Biotin R caused the decay of lichens at the site (Figs. 19, 20). The effect



Fig. 19. Prior to application of 40% solution of Biotin R (photo by M. Gąsior)



Fig. 20. Seven days after application (photo by M. Gąsior)

Table 1. Results of modal analysis in vol. % (elaborated by W. Bartz)

Constituent	Sample number									
	4	5	6	7	8	9	10	11	12	13
Quartz	29.4	66.4	60.1	57.8	68.2	58.8	56.7	62.7	65.4	64.0
Feldspar	0.8	6.3	6.2	6.7	3.7	5.7	5.6	2.8	9.8	5.4
Lithic grains	1.0	4.7	3.0	3.2	3.5	1.7	4.8	1.4	1.9	1.6
Pore	25.0	7.3	5.9	3.5	10.1	16.6	14.5	6.1	9.1	15.7
Cement	43.8	15.3	24.8	28.8	14.5	17.2	18.4	27.0	13.8	13.3

was dependent on the concentration applied – the higher the concentration, the more effective the decay. Unfortunately, within a short period of time, it was found that the disinfected area of the rock was quickly inhabited by other lichen specimens. This is a natural process – the special agent used did not restrain the growth for much longer.

It should also be mentioned that disinfection of the whole rock would require the use of a significant amount of chemicals, which would not be without impact on the natural environment. These types of actions can possibly be recommended only to protect the most valuable petroglyphs.

#### Petrographic and mineralogical analyses

Mineralogical analysis showed the investigated samples are clastic sedimentary rocks sandstones (Fig. 21). Despite a few minor differences, they share a number of common petrographic features. They consist mainly of quartz grains and a lower amount of feldspar and lithic grains (rock fragments) (Table 1). The only exception is sample 4, where the volume of quartz, as well as other aforementioned constituents, is much lower (Table 1). Accessory minerals, including tourmaline and zircon, are very scarce (below 0.1 vol. %).

Rock porosity varies widely, from 3.5 vol.% up to 16.6 vol.% (Table 1). Moreover, there is a clear correlation between porosity and cement volume ( $R = -0.67$ ) as samples with a larger cement volume usually exhibited lower porosity. On the other hand, there is no clear correlation between the total volume of the framework grains and rock porosity ( $R = -0.15$ ). Samples strongly enriched in the framework are depleted in the cement ( $R = -0.63$ ).

Matrix grains ( $<0.06$  mm) occur in very small quantities. Thus, according to the most popular classification of sandstones [17], the rock is quartz arenite (samples 4, 8, 11; Fig. 21) or subarcosic arenite (samples 5, 6, 7, 9, 10, 12, 13; Fig. 21).

The cement in the sandstone is in the form of quartz overgrowth and the black/brown mass seen in plane-polarized light (Fig. 22) is composed of iron-oxide minerals (hematite, goethite) mixed with very fine, plate-like minerals (sericite and/or clay minerals). Their proportion is variable. In many cases, iron-oxide minerals dominate (samples 5, 6, 7, 13), whereas most samples (4, 8, 9, 10, 11, 12) have cement enriched in clay minerals.

Sample 4 is slightly different in comparison to most of the other samples. It exhibited unusually high porosity

and, at the same time, a high content of cement (Table 1). An exact microscopic analysis of the sample showed that it is heavily cracked (Fig. 22) and the framework grains are disseminated in an abundant fine-crystalline mass. The latter shows a yellowish tint, and it is more translucent than typical cement that is seen as black/brown in plane-polarized light. The observed differences presumably result from a significant degree of weathering of the rock.

#### Scanning electron microscopy

Mapping analyses of representative areas of rock samples, as well as point analyses, show that some elements are abundant and relatively evenly distributed in the rock, while others occur in minor amounts and only in places. Moreover, there are some correlations between certain elements. Thus, silicon and oxygen are ubiquitous, while iron, potassium, and aluminium occur less frequently. On this basis, it can be concluded that the vast majority of the framework grains are quartz. The locally observed concentrations of potassium, aluminium, silicon, and oxygen correspond to sparse alkali feldspar grains. The occurrence of aluminium is, as stated above, associated with alkali feldspars, but this element is also located in the intergranular spaces. Its occurrence is associated with the presence of silicon and oxygen bound together in platy clay minerals composed of close kaolinite or montmorillonite

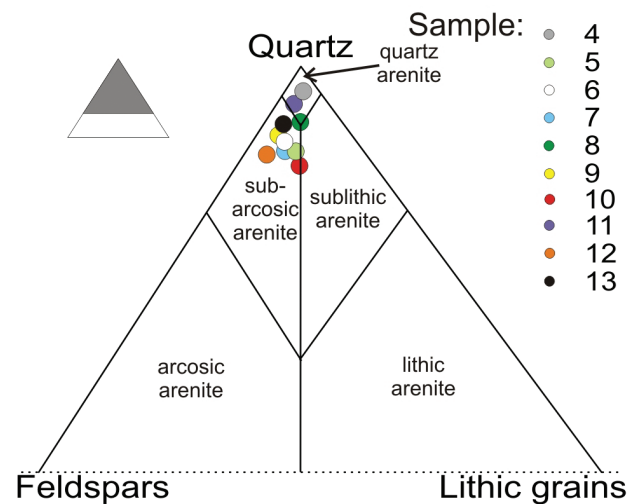


Fig. 21. Classification of investigated Samaipata sandstone samples (elaborated by W. Bartz)

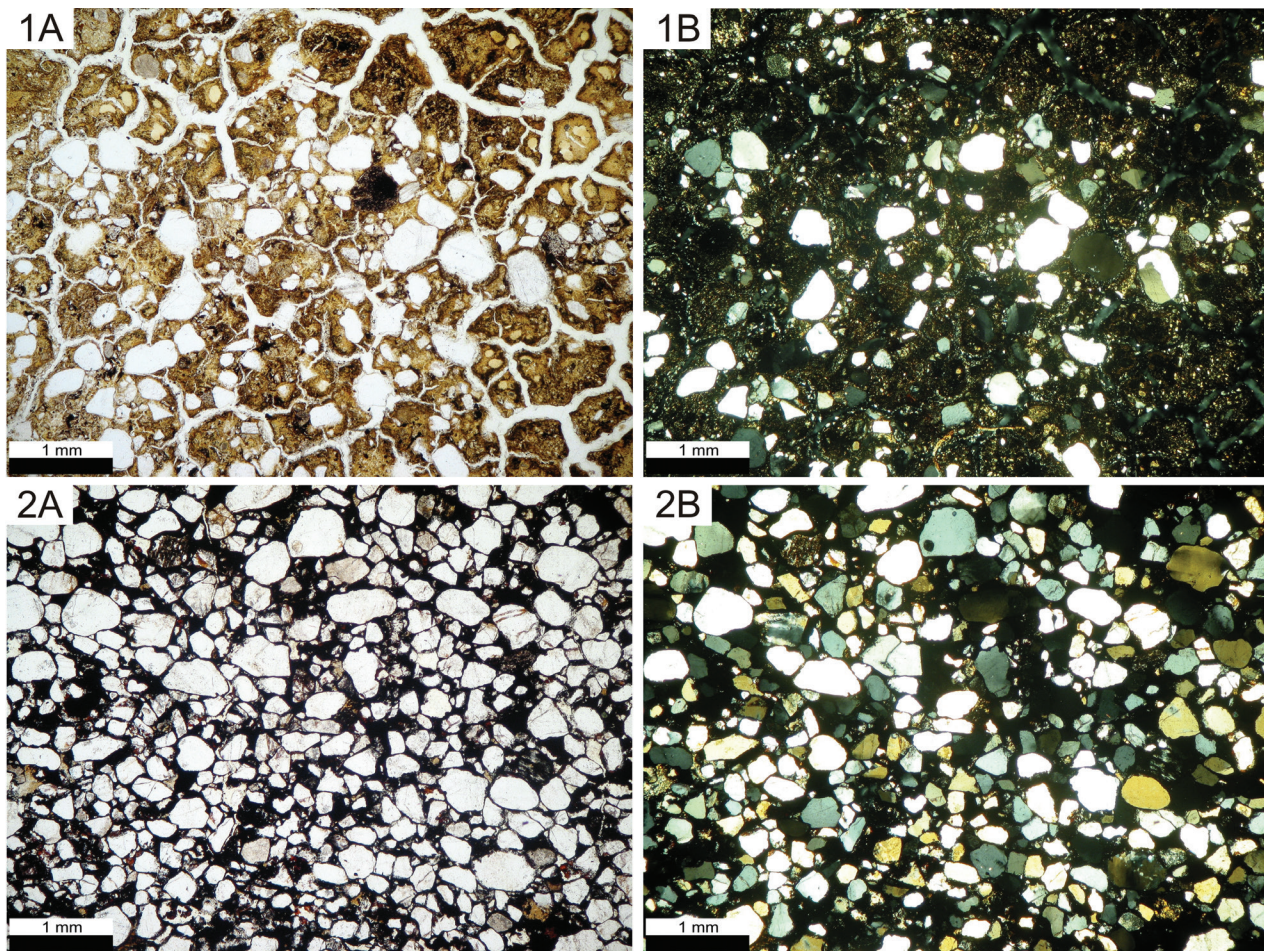


Fig. 22. Samaipata sandstone sample 4 (upper row) and sample 7 (bottom row) viewed in plane-polarized light (A) and cross-polarized light (B) (elaborated by W. Bartz)

(smectite). Sporadically, this kind of platy clay additionally contains small amounts of potassium or iron and magnesium, representing illite, sericite, or chlorite crystals, respectively. The iron is evenly distributed in the intergranular spaces and is associated with oxygen. It indicates that the crystalline mass (the cement) filling the pore spaces between the framework grains contains iron oxide minerals – hematite, limonite, or goethite. Sporadically observed and weak calcium bands found on a few EDS spectra imply the presence of small amounts of calcite.

#### *Thermal analysis*

A strong endothermic effect was visible at 570 °C with no associated weight loss. This was the result of the polymorphic transformation of quartz [18, p. 55], [19]. At temperatures below 100 °C, a strongly marked weight loss was visible on the DTG curve (first derivative of the weight curve), and this is associated with an endothermic effect. It should be interpreted as the process of releasing unbound (hygroscopic) water. Less common (samples 9, 8, and 10) was a poorly marked deflection of DTG and DDSC (first derivative of the heat-flow curve), which was visible slightly above the temperature of 100 °C. This can be interpreted as the process of dehydration of clay mine-

rals (illite and/or smectite) and/or gypsum [18, pp. 83, 76–80, 125]. Another strong weight loss was observed in the temperature range of 200–400 °C. This was accompanied by endothermic effects well marked on the DDSC curve. Within this temperature range, iron oxyhydroxides (goethite, lepidocrocite) undergo dehydroxylation [18, pp. 64, 65], [19, p. 38]. Some of the samples (7, 8, 9, 10) showed additional minor endothermic and weight loss effects within this temperature region. Presumably, this was due to the occurrence of both forms of FeOOH – goethite and lepidocrocite. The dehydroxylation temperature of these minerals differs by several dozen degrees Celsius [18, pp. 64–85]. A very strong weight-loss reaction was also observed at a temperature close to 500 °C, and was accompanied by an endothermic reaction. Clay minerals undergo dehydroxylation at similar temperatures. A very strong weight loss suggests their abundance. Depending on the type of clay mineral, the peak temperature of the weight-loss effect shifts, and for smectite is 680 °C, illite 550 °C, and kaolinite 520–590 °C [18, pp. 68–84], [19, pp. 28–34]. Due to the fact that some of the samples clearly showed reactions below 500 °C, it can be assumed that kaolinite was present in the sample. The split-peak behaviour observed in a few samples suggests an overlapped dissociation of two different phyllosilicates – kaolinite and

illite. Some samples showed a relatively weak weight-loss reaction with the associated endothermic reaction in the temperature range of 630–660 °C. This could be interpreted as the result of the thermal dissociation of calcium carbonates (calcite) with a low degree of crystallinity [18, p. 108].

### X-ray powder diffraction

The results showed the prevailing presence of quartz due to the peaks at 3.34 Å, 4.25 Å, and 1.81 Å (Fig. 24).

Compared to quartz, less intense peaks were attributed to feldspar minerals – microcline and orthoclase, evidenced by stronger peaks: 4.22 Å, 3.26 Å, 3.25 Å and weaker peaks: 3.31 Å, 3.77 Å, 4.22 Å, respectively (Fig. 23). Although the grains of minerals discussed belong to the frameworks and are relatively larger, a small number of the finest fraction (the matrix) might have passed through the sieve.

The next component identified by XRD was iron oxide – hematite, representing the cement of the rock. Its presence is shown by the peaks observed at 2.70 Å, 2.52 Å, and 1.69 Å (Fig. 23).

All of the obtained diffraction patterns are marked with peaks located at low 2Theta values: 10.10 Å, 7.18 Å, and 17.50 Å. They illustrate the presence of clay minerals: illite (or structurally similar muscovite), kaolinite, and smectite, respectively. Illite peaks were also found at 3.35 Å and 5.03 Å, while kaolinite peaks were found at 3.58 Å and 4.33 Å. Peaks located at 4.49 Å and 2.57 Å were attributed to smectite. Aluminium hydroxide (gibbsite) was also identified on the basis of peaks 4.85 Å and 2.38 Å (Fig. 23).

The occurrence of crystalline phases within the analysed samples, identified by means of XRD, was strongly varied. Quartz, alkali feldspar, hematite, illite (and/or muscovite) were found in all samples. Unlike them, gibb-

site was very rare and was only found in sample 10. A frequent constituent was clay minerals – kaolinite, identified in samples 5, 7, 10, and 13 and smectite, found in samples 5, 7, 8, 11, and 13 (Fig. 23).

### Properties of local clay

The clay fraction of the local clay material that could potentially be used for restoration is a mixed-layer mineral – chlorite-smectite, kaolinite, and illite (or structurally similar muscovite; Fig. 24). Illite was identified on the basis of peaks at 10.06 Å, 3.33 Å, and 4.96 Å that remained unaltered by ethylene glycol saturation and heating to 550 °C. Kaolinite peaks were found at 7.21 Å, 3.57 Å, and 4.47 Å in the untreated sample and disappeared when the material was heated to 550 °C. The mixed-layer smectite-chlorite was recognized on the basis of peaks at 14.43 Å, 3.33 Å (overlapping with the most intense quartz peak), and 7.21 Å. The small shift of peak 001 ( $d = 14.43$  Å) after ethylene glycol saturation, visible in the form of a wide peak at 15.5–17.5 Å, confirmed the presence of the smectite layer. This particular peak shifted to 8–10 Å when the sample was heated (Fig. 24).

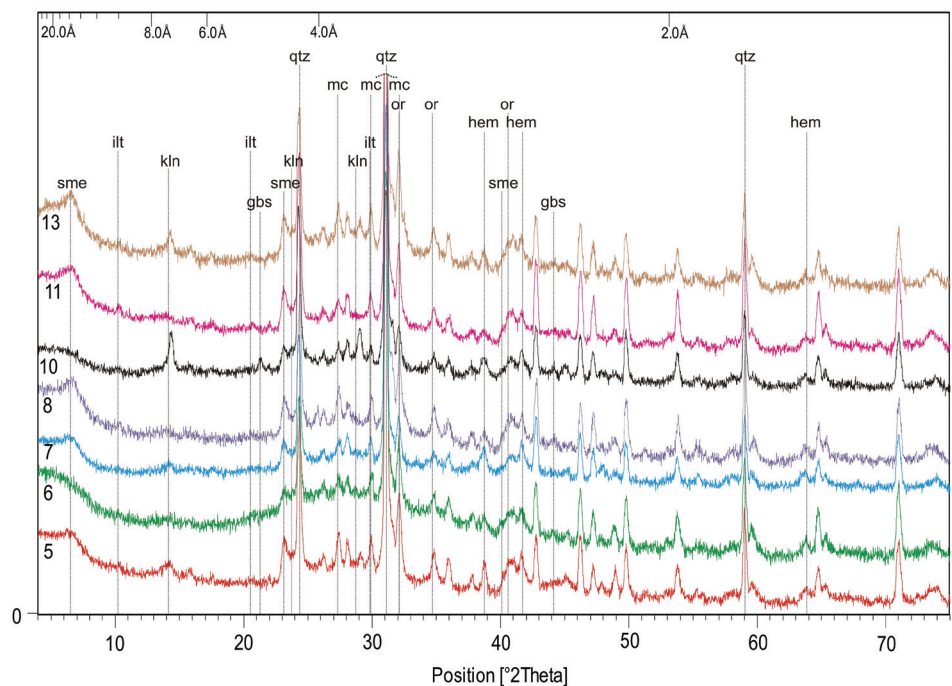
As smectite is known to increase in volume many times when watered and shrink when it dries, local clay is completely unsuitable for conservation purposes. Other clay deposits need to be found, and their properties need to be examined before using.

### General conclusions and limitations

The formulation of strategies and detailed conservation programs is not the purpose of this study. These must be arranged by local specialists familiar with all local administrative and financial conditions, as well as the availability of specific materials and conservation technologies.

Fig. 23. Results of XRD analysis of sieved fraction <0.063 mm.

Mineral abbreviations:  
sme – smectite, ilt – illite,  
qtz – quartz, gbs – gibbsite,  
kln – kaolinite,  
or – alkali feldspar (orthoclase),  
mc – alkali feldspar (microcline),  
hem – hematite  
(elaborated by W. Bartz)



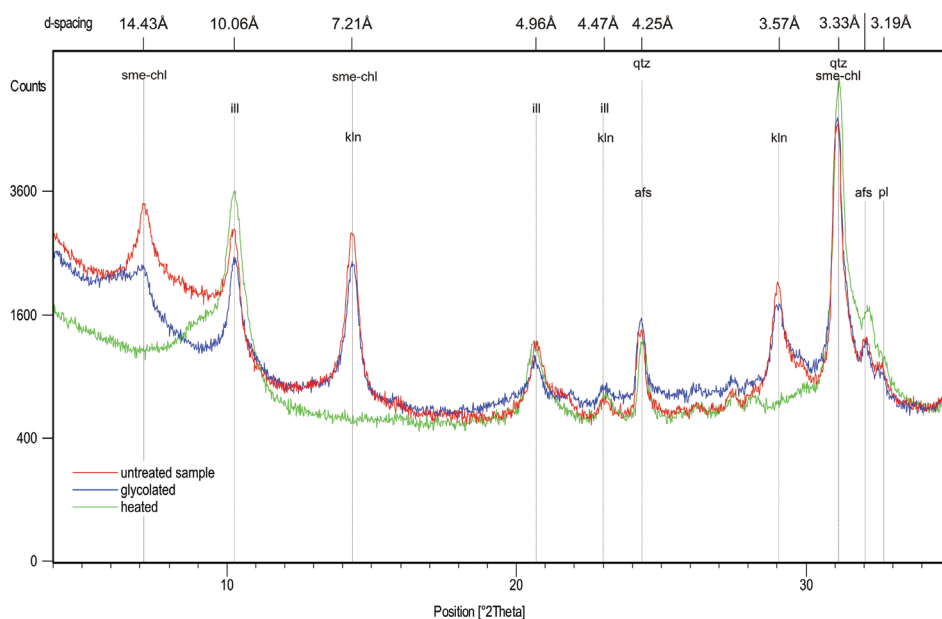


Fig. 24. Results of XRD analysis of oriented clay fraction mounts. Mineral abbreviations: sme-chl – smectite-chlorite, ill – illite, qtz – quartz, kin – kaolinite, afs – alkali feldspar, pl – Ca-Na feldspar (elaborated by W. Bartz)

However, the analyses and data gathered above can be used as a starting point for preparing detailed plans for the long-term preservation of El Fuerte de Samaipata.

One recommendation can already be applied at this stage. In light of the described climatic and topographic factors, as well as the results of petrographic and mineralogical analyses of local sandstone, it is necessary to consider the problem of water retained in local depressions. Two contradictory recommendations can be formulated for this:

– As smectite swells and shrinks, it is not advisable to drain rainwater from all the depressions as soon as possible. Fast and frequent changes (watering and drying) will promote the transformation of a smectite binder, which would increase the volume of smectite and lead to faster erosion of the rock. When considering only smectite, it is advisable to leave the water in the depressions and allow it to slowly evaporate.

Moreover, the contrary:

– The prolonged presence of water promotes the transformation of the hematite binder into a ferric hydroxide gel in the form of soluble oxyhydroxide, which causes faster binder removal. From this point of view, it is essential to drain water from the depressions as soon as possible.

The main part of the binder of Samaipata rock is hematite, and its dissolution seems to be the main reason for the erosion of the rock.

Considering both recommendations and the reasons behind them, it seems more important to drain water from all depressions as soon as possible.

The size of the rock, its construction, chemical composition, position/location, and the multitude of destructive agents to which it is exposed create a combination of factors that do not allow effective conservation and maintenance procedures to be conducted that would adequately protect this natural monument from destruction. Only small-scale activities are possible for selected parts of El Fuerte. One of the actions that could be taken and which would delay the erosion of this valuable and unique monument is to fill the main cracks in the rock that intensify erosion by allowing water to infiltrate the rock. For this purpose, it is possible to use mineral fillers and binders recommended for the maintenance and conservation of stone monuments [20]. This work should be carried out as a separate project under the guidance of an experienced stone conservator and preceded by careful research and tests on the use and application of suitable fillers and binders.

### References/Bibliografía

- [1] De Alcaya D., *Relación cierta* [1636], [in:] I. Combès, V. Tyuleneva (eds.), *Paititi. Ensayos y documentos*, Editorial Itinerarios, Cochabamba 2011, 240–251.
- [2] Ponce Sanginés C., *Alcides d'Orbigny y su viaje a Samaipata en 1832*, [in:] R.D. Arze Aguirre (dir.), *El naturalista francés, Alcide Dessaline d'Orbigny en la visión de los bolivianos*, Institut Français d'Études Andines, Plural editores, Lima–La Paz 2002 [1975], 307–315.
- [3] Nordenskiöld E., *Forschungen und Abenteuer in Südamerika*, Strecker und Schroder, Stuttgart 1924.
- [4] Pucher L., *Ensayo sobre el arte prehistórico de Samaypata*, “Revista de la Universidad de San Francisco Xavier”, Universidad Mayor de San Francisco Xavier Sucre, Sucre 1945.
- [5] Alcázar de La Fuente R., *El Sitio Ceremonial y Administrativo de El Fuerte de Samaipata*, “Tesape Arandu” 2015, Año 4, N° 21, 1–9.
- [6] Trimbom H., *Der skulptierte Berg von Samaipata*, “Archäologische Studien in den Kordilleren Boliviens”, Bd. 3, “Baessler Archiv, Beiträge zur Völkerkunde” 1967, NF 5, 130–169.
- [7] Meyers A., *Trabajos Arqueológicos en Samaipata, Departamento de Santa Cruz, Bolivia, Primera Temporada 1992*, “Boletín SIARB” 1993, N° 7, 48–58, <http://siarb-bolivia.org/wp-content/uploads/2019/08/bol7a.pdf>.
- [8] Meyers A., *Las Campañas Arqueológicas en Samaipata 1994–1996. Segundo Informe de Trabajo*, “Boletín SIARB” 1998, N° 12, 59–86.

- [9] Meyers A., *Reflexiones acerca de la periodización de la Cultura Inka: perspectivas desde Samaipata, Oriente de Bolivia*, [in:] C. Diez Marín (ed.), *Actas del XII Congreso Nacional de Arqueología Argentina*, Editorial de la Universidad de la Plata, La Plata 1999, t. 1, 239–251.
- [10] *El Fuerte de Samaipata: Estudios arqueológicos*, A. Meyers, I. Combès (comp.), Biblioteca del Museo de Historia Universidad Autónoma Gabriel René Moreno, Santa Cruz de la Sierra 2015.
- [11] Combès I., Meyers A., *El Fuerte de Samaipata en contexto: Estudios históricos*, Biblioteca del Museo de Historia Universidad Autónoma Gabriel René Moreno, Santa Cruz de la Sierra 2018.
- [12] Avilés S., *Conservazione del tempio della rocca scolpita di Samaipata – Santa Cruz, Bolivia (Sudamerica)*, Tesi di Master: Università di Bologna, Sede di Ravenna, Facoltà di Conservazione dei Beni Culturali, Dipartimento di Storie e Metodi per la Conservazione dei Beni Culturali, 2002, [www.stonewatch.de/media/download/sc%2004.pdf](http://www.stonewatch.de/media/download/sc%2004.pdf) [accessed: 27.09.2017].
- [13] Avilés S., *Introduzione alla conservazione della Rocca Scolpita di Samaipata, Bolivia*, 2011, <http://www.rupestreweb.info/samaipata.html> [accessed: 27.09.2017].
- [14] Avilés S., *La conservación de la Roca Sagrada de Samaipata*, [in:] A. Meyers, I. Combès (comp.), *El Fuerte de Samaipata: Estudios arqueológicos*, Biblioteca del Museo de Historia Universidad Autónoma Gabriel René Moreno, Santa Cruz de la Sierra 2015, 161–170.
- [15] Elsen J., *Microscopy of historic mortars – a review*, “Cement and Concrete Research” 2006, Vol. 36, Iss. 8, 1416–1424.
- [16] Strzelczyk A.B., Karbowska-Berent J., *Drobnoustroje i owady niszczące zabytki i ich zwalczanie*, Wydawnictwo Naukowe UMK, Toruń 2004.
- [17] Pettijohn F.J., Potter P.E., Siever R., *Sand and sandstone*, Springer-Verlag, Berlin–Heidelberg–New York 1972.
- [18] Földvári M., *Handbook of thermogravimetric system of minerals and its use in geological practice*, Magyar Állami Földtani Intézet (Geological Institute of Hungary), Budapest 2011.
- [19] Wyrwicki R., *Analiza derywograficzna skał ilastych*, Wydawnictwo Uniwersytetu Warszawskiego, Warszawa 1988.
- [20] Łukaszewicz J.W., *Rodzaje kamieni sztucznych, właściwości oraz odporność na działanie czynników niszczących*, [in:] W. Domasłowski (red.), *Zabytki kamienne i metalowe ich niszczenie i konserwacja profilaktyczna*, Wydawnictwo Naukowe UMK, Toruń 2011, 47–87.

### Acknowledgements/Podziękowania

The presented work is a part of the research project sponsored by the grant given to the Wrocław University of Science and Technology by the Polish National Science Centre (grant No. 2014/15/B/HS2/01108). Additionally, the municipality of Samaipata, represented by Mayor Falvio López Escalera, contributed to this research by providing the accommodation during the fieldwork in June and July 2016, as well as in

July 2017. The Ministry of Culture and Tourism of Bolivia kindly granted all necessary permits (UDAM No. 014/2016; UDAM No. 060/2017). The research was conducted in close cooperation with the Centre for Pre-Columbian Studies of the University of Warsaw in Cusco. Specialists from many other universities and research centres also joined the project.

### Abstract

El Fuerte de Samaipata is a pre-Hispanic archaeological site in Bolivia that has been on the UNESCO World Heritage List. Its main part – the rock – is densely covered with a complex arrangement of terraces, platforms, water reservoirs, channels, and petroglyphs. The rapidly progressing erosion of the rock is making the petroglyphs less and less clear, and some are no longer recognisable. The main topic of this study is to indicate all risk factors conducive to erosion and to create risk maps identifying the most vulnerable areas that require immediate conservation intervention. Parallel mineralogical and petrographic studies show that the Samaipata rock is a quartz-rich, porous, well-sorted sandstone, classified as quartz arenite or subarcosic arenite. The cement of the rock is composed of quartz overgrowth and ubiquitous, pore-filling hematite-clay aggregates containing non-expanding kaolinite, illite, and expanding smectite. The rock exhibits different stages of weathering, from relatively fresh to strongly altered and heavily cracked. In comparison to fresh rock, the latter has cement enriched in clay minerals and is depleted in hematite due to weathering and the dissolution of the iron-bearing phase.

**Key words:** Samaipata, conservation, climatic and topographical risk factors, sandstone, mineralogy

### Streszczenie

El Fuerte de Samaipata to wpisane na Listę Światowego Dziedzictwa UNESCO prehiszpańskie stanowisko archeologiczne w Boliwii. Jego główna część to skała ze złożonym układem tarasów, platform, zbiorników wodnych, kanałów i petroglifów. Szybko postępująca erozja sprawia, że petroglify stają się coraz mniej wyraźne, a niektóre nie są już rozpoznawalne. Głównym tematem badań jest wskazanie wszystkich czynników ryzyka sprzyjających erozji oraz stworzenie map ryzyka identyfikujących najbardziej wrażliwe obszary wymagające natychmiastowej interwencji konserwatorskiej. Badania mineralogiczne i petrograficzne wskazują, że Samaipata to bogaty w kwarc, porowaty, dobrze posortowany piaskowiec, sklasyfikowany jako arenit kwarcowy lub arenit subarkozowy. Spoiwo składa się z przerostu kwarcu i wszechobecnych, wypełniających pory agregatów hematytowo-gliniastych zawierających nierozprężający się kaolinit, illit i rozszerzający się smektyt. Skała wykazuje różne etapy wietrzenia, od stosunkowo świeżego do mocno zmienionego i mocno spękanego. W porównaniu ze świeżą skałą ta ostatnia ma cement wzbogacony w minerały ilaste i jest zubożona w hematyt z powodu wietrzenia i rozpuszczenia fazy żelazonośnej.

**Słowa kluczowe:** Samaipata, konserwacja, klimatyczne i topograficzne czynniki ryzyka, piaskowiec, mineralogia



Documenting petroglyphs  
(photo by M. Ziolkowski)  
Dokumentowanie petroglifów  
(fot. M. Ziolkowski)